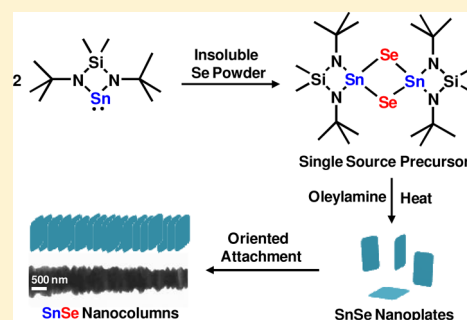


## Colloidal Synthesis of SnSe Nanocolumns through Tin Precursor Chemistry and Their Optoelectrical Properties

Kwonho Jang,<sup>†</sup> In-yeal Lee,<sup>‡</sup> Juan Xu,<sup>†</sup> Jaewon Choi,<sup>†</sup> Jaewon Jin,<sup>†</sup> Ji Hoon Park,<sup>†</sup> Hae Jin Kim,<sup>§</sup> Gil-Ho Kim,<sup>\*,‡</sup> and Seung Uk Son<sup>\*,†</sup><sup>†</sup>Department of Chemistry and Department of Energy Science, Sungkyunkwan University, Suwon 440-746, Korea<sup>‡</sup>School of Electronic and Electrical Engineering, and Sungkyunkwan University Advanced Institute of Nanotechnology (SAINT), Sungkyunkwan University, Suwon 440-746, Korea<sup>§</sup>Korea Basic Science Institute, Daejeon 350-333, Korea

## Supporting Information

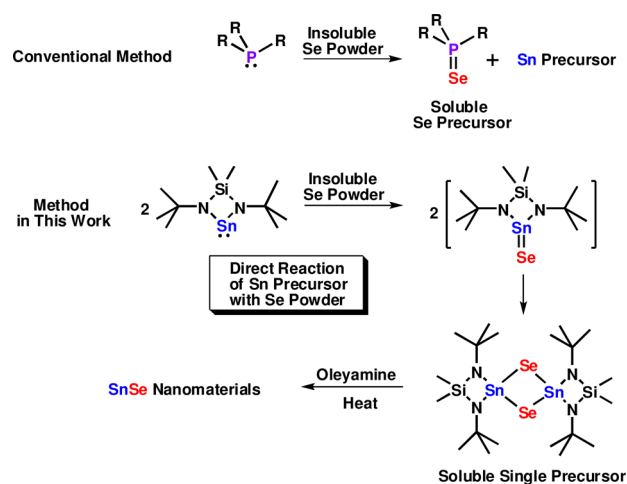
**ABSTRACT:** Through tin precursor chemistry, SnSe nanocrystals were phase-selectively prepared. Monomeric N-heterocyclic stannylene,  $[\text{Me}_2\text{Si}(\text{N}^t\text{Bu})_2\text{Sn}]$ , having lone pair electrons, was prepared by a literature method, and it had a direct reactivity toward selenium powder. The resultant dimerized compound with a 1:1 stoichiometric ratio of Sn to Se was used as a precursor to synthesize tin selenides. Thermolysis of the precursor solution in oleylamine resulted in SnSe plates. The oriented attachment of SnSe plates through (100) crystalline planes formed the SnSe nanocolumns, which were characterized by SEM, TEM, PXRD, EDS, and XPS. The indirect band gap of the SnSe nanocolumns was red-shifted, compared with those of SnSe plates. The SnSe nanocolumns showed an increased photocurrent under visible light irradiation. We believe that similar precursor chemistry in this work can be further extended to group IVA elements.



During the last two decades, there has been great progress in colloidal synthesis of semiconductor nanocrystals.<sup>1</sup> Especially, diverse metal chalcogenides have been prepared extensively. In the case of metal selenides, the studies over the last two decades have focused on several privileged metal selenides such as CdSe, ZnSe, and PbSe.<sup>1,2</sup> However, more exploration should definitely be conducted on more diverse metal selenides. In conventional colloidal synthesis for metal sulfides, soluble sulfur powder has been used frequently as a sulfide precursor and has shown numerous successful results.<sup>3</sup> However, in synthetic cases of metal selenides, use of selenium powder has been limited because of its very poor solubility.<sup>4</sup> Thus, selenium powder was first reacted with electron-rich phosphines such as trioctylphosphine, and the resultant soluble phosphine selenide has been used as a selenide precursor<sup>5</sup> (Scheme 1). Interestingly, several groups have very recently reported on the colloidal synthesis of tin selenide nanomaterials using trioctylphosphine selenide.<sup>6</sup> Although this method has been widely used, phosphines are basically expensive, toxic, and sensitive to air. Thus, alternative synthetic methods without use of phosphines have been sought.<sup>7</sup> For example, our research group has used imidazoline-2-selenone as a new soluble selenide precursor based on N-heterocyclic carbene chemistry.<sup>8</sup> However, if the counterpart precursor of selenide has a direct reactivity toward insoluble selenium powder, it would be a more interesting and efficient strategy.

Tin selenides have intriguing optoelectrical properties and have been applied as light harvesting layers in solar cells.<sup>6</sup> However, in the synthesis of tin selenide materials, phase

## Scheme 1. Comparison of the Conventional Synthetic Method with the New One in This Work for Colloidal Tin Selenide Nanomaterials



problems have often been encountered. The two main phases of tin selenides are SnSe<sup>6</sup> and SnSe<sub>2</sub>.<sup>8a</sup> For example, in our previous report, although we used the Sn(II)Cl<sub>2</sub> and the tailored soluble selenide precursor, SnSe<sub>2</sub> materials were

Received: April 28, 2012

Revised: May 30, 2012

Published: June 14, 2012

exclusively obtained, instead of the expected SnSe.<sup>8a</sup> Although tedious screening of reaction conditions can result in phase-selective tin selenide materials, an appropriate precursor chemistry can be devised to obtain selectively the target materials.

N-Heterocyclic stannylenes such as  $[\text{Me}_2\text{Si}(\text{N}^t\text{Bu})_2\text{Sn}]$  with lone pair electrons on Sn are known and can be prepared *via* reaction of the dilithiated species of  $(^t\text{BuNH})_2\text{SiMe}_2$  with  $\text{Sn}(\text{II})\text{Cl}_2$ <sup>9</sup> (Scheme 1). These tin compounds with lone pair electrons on Sn have a similar reactivity to that of well-developed trialkylphosphine with lone pair electrons on phosphine, toward selenium powder. It was reported that they finally form dimerized compounds with a 1:1 stoichiometric ratio of Sn to Se.<sup>9b</sup> Thus, it can be speculated that the use of these dimerized compounds as a single precursor could result in SnSe materials in colloidal synthesis of tin selenides.

In addition to phase control of nanocrystals, their shape-controlled synthesis has been an interesting issue because certain physical properties are closely related to the shapes of materials.<sup>1</sup> While a kinetic control of the growing crystalline planes by surfactants has been frequently applied for shape-controlled synthesis of nanocrystals, the connection of the nanobuilding blocks also can induce an anisotropic shape evolution. A representative example is the oriented attachment process of isotropic nanobuilding blocks to 1D materials.<sup>10</sup> While the oriented attachment process has been frequently observed in the growth of inorganic materials, the attachment of 2D materials is relatively rare for two main reasons.<sup>11</sup> First, attaching plates in a side by side manner is kinetically difficult because of the thinness of the plates. Second, the top or bottom planes of 2D plates have a relatively low reactivity for further growth as a result of the strong interaction of surfactants. However, in certain reaction situations, 2D materials can show an oriented attachment of plane to plane that results in so-called nanocolumns.<sup>11</sup> Although known cases are relatively rare, several examples of the nanocolumns have been reported.<sup>11</sup> Our research group has continued the studies on the colloidal synthesis of 2D nanomaterials.<sup>3,8</sup> In this work, we report the preparation of SnSe nanocolumns through an oriented attachment of plates and their optoelectrical properties.

In a typical synthetic procedure for SnSe nanocolumns, a tin precursor compound,  $[\text{Me}_2\text{Si}(\text{N}^t\text{Bu})_2\text{Sn}]$ ,<sup>9</sup> was reacted with selenium powder in diethyl ether under argon. In this process, insoluble selenium powder was gradually dissolved into solution to form a transparent solution. The precursor solution was added to oleylamine, and the reaction mixture was heated at 220 °C for 1 h. After being cooled to room temperature, the reaction mixture was poured into excess methanol. The resultant precipitates were retrieved by centrifugation. After being washed with methanol three times, the resultant precipitates were dried under vacuum for 1 day. The powder was investigated by scanning (SEM) and transmission electron microscopy (TEM).

As shown in the SEM images in Figure 1a and the TEM image in Figure 1b, the materials consisted of packed plates with 1D character. The average diameter and length of nanocolumns were measured as  $810 \pm 110$  nm and  $\sim 10$   $\mu\text{m}$ , respectively. The thicknesses of plates were in the range 70–100 nm. High resolution (HR) TEM analysis revealed that the nanocolumns were elongated in the [100] direction of the orthorhombic SnSe materials, showing a unique double-layered crystal structure<sup>6a,c,12</sup> (Figure 1c). It is noteworthy that the (100) planes of orthorhombic SnSe materials have a relatively

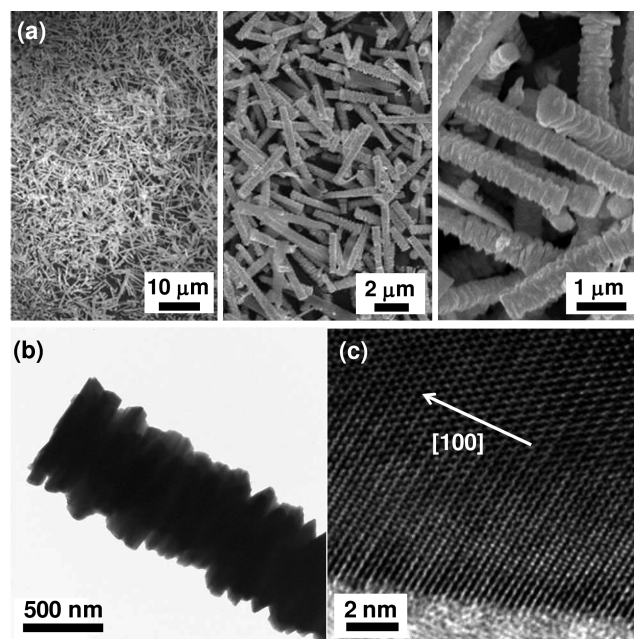


**Figure 1.** (a) SEM, (b) TEM, and (c) HR-TEM images of SnSe nanocolumns.

weak bonding with each other.<sup>6b</sup> Powder X-ray diffraction (PXRD) studies showed that all PXRD peaks perfectly match with those of orthorhombic SnSe materials (JCPDS # 48-1224) (Figure 3e). Energy dispersive X-ray spectroscopy (EDS) supports the 1:1 stoichiometric ratio of Sn to Se (Figure 2a).

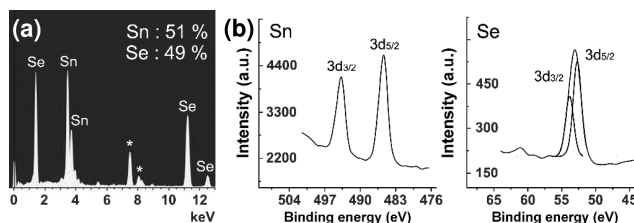


**Figure 2.** (a) EDS spectrum (the peaks indicated by asterisks correspond to Ni from the TEM grid) and (b) XPS spectra of the Sn d orbital and the Se d orbital of SnSe nanocolumns.

The X-ray photoelectron spectroscopy (XPS) showed Sn  $3d_{3/2}$  and  $3d_{5/2}$  orbital peaks at 493.8 and 485.4 eV, respectively, and Se 3d orbital peaks at 53.1 eV, which match well with those of SnSe materials.<sup>13</sup>

To get information pertaining to the growth mechanism, the materials were taken at 20, 40, and 60 min after the reaction temperature reached 220 °C and were investigated by SEM, TEM, and PXRD studies. As shown in Figure 3a–c, in the early stage, plates predominantly were observed; then, 1D materials gradually appeared. Finally, 1D rods consisting of the packed 2D materials predominantly were observed. In addition, PXRD peaks became sharper (Figure 3e). The growth mechanism can be displayed as in Figure 3d, which shows the formation of 1D materials by the oriented attachment of plates.

For further characterization of the orientation of crystalline planes, TEM-electron diffraction (ED), HR-TEM, and PXRD studies were conducted on the SnSe nanoplates (Figure 4). In HR-TEM analysis on the top-view of SnSe nanoplates, the {011} set of planes with 0.30 nm interplane distance were predominantly observed (Figure 4c). In the ED pattern, HR-

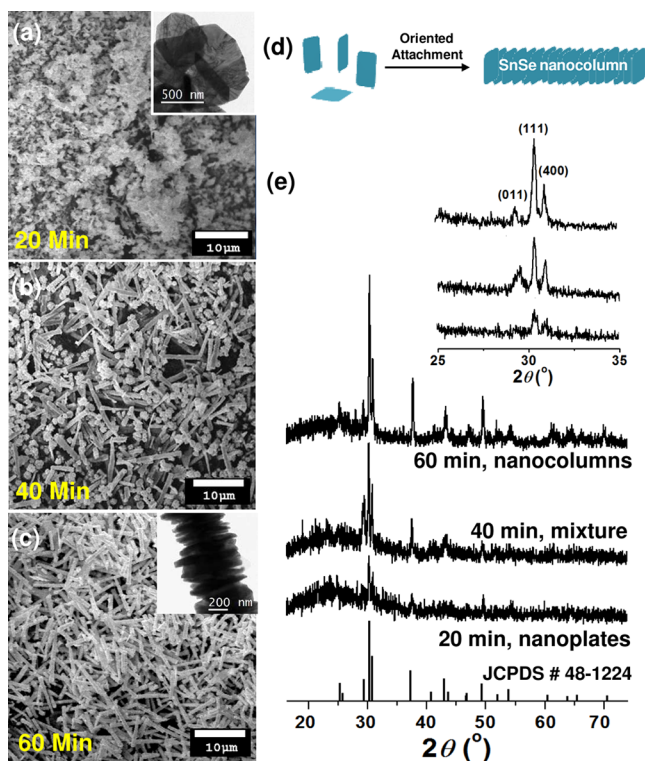


**Figure 3.** SEM and TEM images of materials taken at 20 min (a), 40 min (b) and 60 min (c) after the reaction temperature reached 220 °C; (e) their PXRD patterns; (d) an illustration of the formation of SnSe nanocolumns by oriented attachment of plates.

TEM analysis, and TEM image of SnSe nanoplates, the 92° angle in the intersection of the {011} set of planes was observed, as reported in the literature on 2D SnSe nanocrystals.<sup>6a</sup> (Figure 4a–c). Compared with the PXRD pattern of

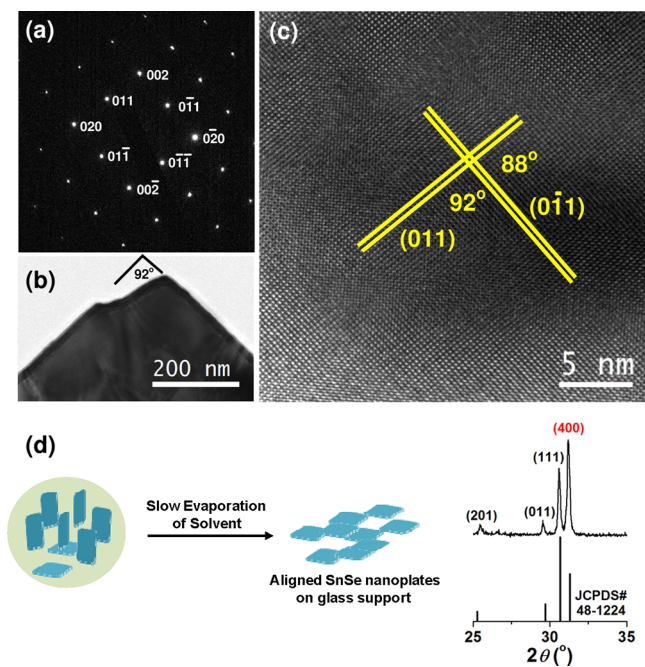


**Figure 4.** (a) ED pattern and (b) TEM and (c) HR-TEM images of SnSe nanoplates and (d) an illustration of the aligned SnSe nanoplates and the corresponding PXRD pattern with an enhanced (400) peak.

bulky SnSe materials, that of the aligned SnSe nanoplates on glass showed enhanced (400) and (800) peaks, which indicates the preferential orientation of plates in the [100] direction<sup>6a</sup> (Figure 4d and Figure S1 in the Supporting Information).

Bulk SnSe is a narrow band gap (~0.9 eV, mid-IR indirect band gap) semiconducting material.<sup>6</sup> Thus, it can be applied as a light absorber in solar cell devices.<sup>6</sup> Considering this, we investigated the optical and optoelectrical properties of SnSe nanocolumns, in comparison with those of SnSe nanoplates. As shown in Figure 5a, the reflectance spectrum of SnSe

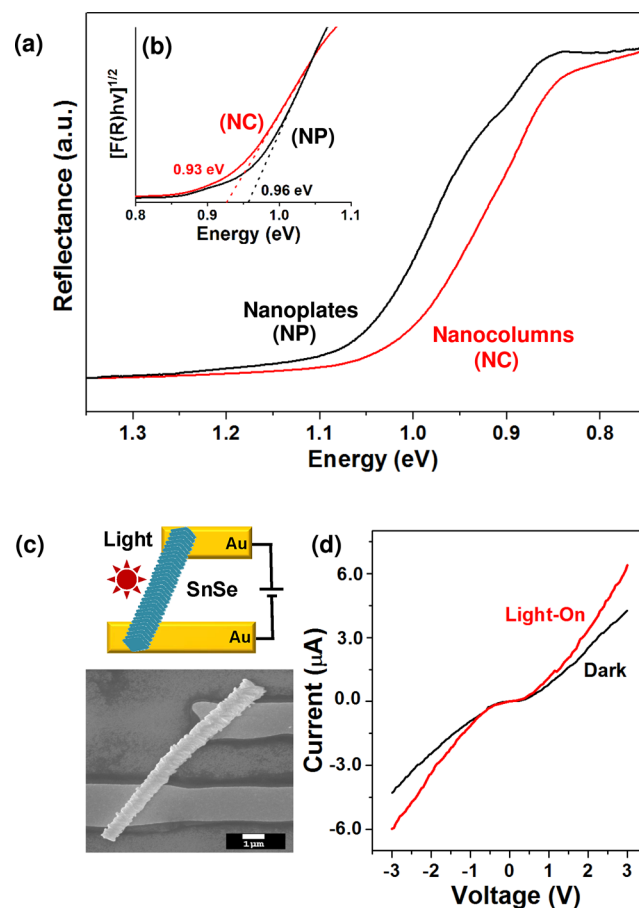


**Figure 5.** (a) Reflectance spectra, (b) plots for the indirect band gap of SnSe nanocolumns and nanoplates, (c) illustration of the device structure for the photocurrent measurement of SnSe nanocolumns and the corresponding SEM image, and (d) optoelectrical properties of SnSe nanocolumns.

nanocolumns was red-shifted, compared with that of the nanoplates. The indirect band gaps of SnSe nanocolumns and nanoplates were obtained from their reflectance spectra by plotting  $[F(R)h\nu]^{1/2}$  versus energy, respectively<sup>6a</sup> (Figure 5b). The obtained band gap value (0.96 eV) of the SnSe nanoplates in this work was nearly the same as that of SnSe nanoplates recently reported in the literature,<sup>6a</sup> and it was significantly blue-shifted from the simulated band gap (0.9 eV) of the bulky SnSe.<sup>14</sup> In comparison with the band gap (0.96 eV) of nanoplates, that of SnSe nanocolumns was red-shifted to 0.93 eV.

To investigate the optoelectrical properties, the SnSe nanocolumn was loaded on Au electrodes prepared through photolithography (Figure 5c).<sup>15</sup> The Au electrodes were separated by 2 μm. In the photocurrent measurements, the

SnSe nanocolumns showed an increase of the photocurrent by ~1.5 times under visible light irradiation from an Xe lamp (wavelength > 420 nm),<sup>16</sup> compared with that observed in the dark state (Figure Sd).

In conclusion, using monomeric N-heterocyclic stannylene, the SnSe nanocrystals were phase-selectively prepared. Tin compound [Me<sub>2</sub>Si(N<sup>t</sup>Bu)<sub>2</sub>Sn:] with lone pair electrons showed direct reactivity toward insoluble selenium powder, forming a dimerized compound with a 1:1 stoichiometric ratio of Sn to Se. The thermolysis of the precursor solution resulted in SnSe plates. The oriented attachment of SnSe plates during the aging process formed SnSe nanocolumns. The band gap of SnSe nanocolumns was red-shifted, compared with that of SnSe nanoplates. The SnSe nanocolumns showed promising optoelectrical properties. We believe that similar precursor chemistry could be further extended to other group IVA elements.

## ■ ASSOCIATED CONTENT

### Supporting Information

General information and detailed procedures of experiments. This material is available free of charge via the Internet at <http://pubs.acs.org>.

## ■ AUTHOR INFORMATION

### Corresponding Author

\*E-mail address: [sson@skku.edu](mailto:sson@skku.edu); [ghkim@skku.edu](mailto:ghkim@skku.edu)

### Notes

The authors declare no competing financial interest.

## ■ ACKNOWLEDGMENTS

This work was supported by Grants NRF-2009-0064488 through the National Research Foundation of Korea funded by the Ministry of Education, Science and Technology. J.H.P. thanks for Grants NRF-2011-0031392 (Priority Research Centers Program) and R31-2008-10029 (WCU program). H.J.K. acknowledges the Hydrogen Energy R Center, a 21st century Frontier R Program. G.H.K. is grateful for Grants R32-2008-10204 (WCU program).

## ■ REFERENCES

- (1) Recent reviews: (a) Talapin, D. V.; Lee, J.-S.; Kovalenko, M. V.; Shevchenko, E. V. *Chem. Rev.* **2010**, *110*, 389. (b) Daniel, M. C.; Astruc, D. *Chem. Rev.* **2004**, *104*, 293. (c) Klabunde, K. J., Ed. *Nanoscale Materials in Chemistry*; Wiley, New York, 2001.
- (2) Representative literature: (a) Peng, X.; Manna, L.; Yang, W. D.; Wickham, J.; Scher, E.; Kadavanich, A.; Alivisatos, A. P. *Nature* **2000**, *404*, 59. (b) Steckel, J. S.; Coe-Sullivan, S.; Bulovic, V.; Bawendi, M. G. *Adv. Mater.* **2003**, *15*, 1862. (c) Li, L. S.; Pradhan, N.; Wang, Y.; Peng, X. *Nano Lett.* **2004**, *4*, 2261.
- (3) Selected examples: (a) Park, K. H.; Jang, K.; Son, S. U. *Angew. Chem., Int. Ed.* **2006**, *45*, 4608. (b) Park, K. H.; Choi, J.; Kim, H. J.; Lee, J. B.; Son, S. U. *Chem. Mater.* **2007**, *19*, 3861. (c) Park, K. H.; Choi, J.; Kim, H. J.; Kim, D.-H.; Oh, D.-H.; Ahn, J. R.; Son, S. U. *Small* **2008**, *4*, 945. (d) Xu, J.; Jang, K.; Jung, I. G.; Kim, H. J.; Oh, D.-H.; Ahn, J. R.; Son, S. U. *Chem. Mater.* **2009**, *21*, 4347.
- (4) Selenium powder is insoluble in conventional organic solvents including oleylamine at ambient temperature. However, there are examples of the successful synthesis of metal selenide nanomaterials using Se powder. (a) Deka, S.; Genovese, A.; Zhang, Y.; Miszta, K.; Bertoni, G.; Krahne, R.; Giannini, C.; Manna, L. *J. Am. Chem. Soc.* **2010**, *132*, 8912. (b) Ithurria, S.; Tessier, M. D.; Mahler, B.; Lobo, R. P. S. M.; Dubertret, B.; Efron, A. L. *Nat. Mater.* **2011**, *10*, 936.

(5) Selected examples: (a) Peng, Z. A.; Peng, X. *J. Am. Chem. Soc.* **2001**, *123*, 183. (b) Owen, J. S.; Chan, E. M.; Liu, H.; Alivisatos, A. P. *J. Am. Chem. Soc.* **2010**, *132*, 18206.

(6) (a) Vaughn, D. D., II; In, S.-I.; Schaak, R. E. *ACS Nano* **2011**, *5*, 8852. (b) Baumgardner, W. J.; Choi, J. J.; Lim, Y.-F.; Hanrath, T. *J. Am. Chem. Soc.* **2010**, *132*, 9519. (c) Liu, S.; Guo, X.; Li, M.; Zhang, W.-H.; Liu, X.; Li, C. *Angew. Chem., Int. Ed.* **2011**, *50*, 12050.

(7) Franzman, M. A.; Schlenker, C. W.; Thompson, M. E.; Brutchey, R. L. *J. Am. Chem. Soc.* **2010**, *132*, 4060.

(8) (a) Choi, J.; Jin, J.; Jung, I. G.; Kim, J. M.; Kim, H. J.; Son, S. U. *Chem. Commun.* **2011**, *47*, 5241. (b) Choi, J.; Kang, N.; Yang, H. Y.; Kim, H. J.; Son, S. U. *Chem. Mater.* **2010**, *22*, 3586.

(9) (a) Veith, M. *Angew. Chem., Int. Ed.* **1975**, *14*, 263. (b) Veith, M.; Nötzel, M.; Huch, V. Z. *Anorg. Allg. Chem.* **1994**, *620*, 1264. (c) Al-Rafia, S. M. I.; Lummis, P. A.; Ferguson, M. J.; McDonald, R.; Rivard, E. *Inorg. Chem.* **2010**, *49*, 9709.

(10) (a) Penn, R. L.; Banfield, J. F. *Science* **1998**, *281*, 969. (b) Penn, R. L.; Banfield, J. F. *Am. Mineral.* **1998**, *83*, 1077. Recent selected examples: (c) O'Sullivan, C.; Gunning, R. D.; Sanyal, A.; Barrett, C. A.; Geaney, H.; Laffir, F. R.; Ahmed, S.; Ryan, K. M. *J. Am. Chem. Soc.* **2009**, *131*, 12250. (d) Koh, W.; Bartnik, A. C.; Wise, F. W.; Murray, C. B. *J. Am. Chem. Soc.* **2010**, *132*, 3909. (e) Wang, Z.; Schliehe, C.; Wang, T.; Nagaoka, Y.; Cao, Y. C.; Bassett, W. A.; Wu, H.; Fan, H.; Weller, H. *J. Am. Chem. Soc.* **2011**, *133*, 14484.

(11) (a) Tian, Z. R.; Voigt, J. A.; Liu, J.; Mckenzie, B.; Mcdermott, M. *J. Am. Chem. Soc.* **2002**, *124*, 12954. (b) Tian, Z. R.; Voigt, J. A.; Mckenzie, B.; Mcdermott, M. J.; Rodriguez, M. A.; Konishi, H.; Xu, H. *Nat. Mater.* **2003**, *2*, 821. (c) Taubert, A.; Kübel, C.; Martin, D. C. *J. Phys. Chem. B* **2003**, *107*, 2660. (d) Viravaidya, C.; Li, M.; Mann, S. *Chem. Commun.* **2004**, 2182. (e) Coudun, C.; Hochepped, J.-F. *J. Phys. Chem. B* **2005**, *109*, 6069. (f) Bai, J.; Qin, Y.; Jiang, C.; Qi, L. *Chem. Mater.* **2007**, *19*, 3367.

(12) Makinistian, L.; Albanesi, E. A. *Phys. Status Solidi B* **2009**, *246*, 183.

(13) Moulder, J. F.; Stickle, W. F.; Sobol, P. E.; Bomben, K. D. *Handbook of X-ray Photoelectron Spectroscopy*; Physical Electronics, Inc.: 1992.

(14) Lefebvre, I.; Szymanski, M. A.; Olivier-Fourcade, J.; Jumas, J. C. *Phys. Rev. B* **1998**, *58*, 1896.

(15) See the Supporting Information for detailed procedures.

(16) The light with wavelengths below 420 nm was cut off with an optical filter. A Xe lamp (200 W) was used as a light source.